Preprints of the 21st IFAC World Congress (Virtual)
Berlin, Germany, July 12-17, 2020

Application of the H_∞ control theory to space missions in engineering education

David Henry *

* *IMS-Lab, Univ. Bordeaux, Bordeaux INP, CNRS (UMR 5218), 351 cours de la libration, 33405 Talence, France (david.henry@ims-bordeaux.fr)*

Abstract: This paper is a training paper for aerospace engineering education *. Its aim is to give the necessary backgrounds for the application of the mixed-sensitivity approach of the robust H_∞ control theory, to space missions. As a support example, the auto-landing phase of a re-entry mission is considered. The considered re-entry vehicle is the HL-20. The paper covers all the aspects of the engineer exercise, i.e. from establishing the non-linear model of the vehicle, considering especially the aerodynamic coefficients, until the implementation of the robust H_∞ controller in the simulator, with a graphical interfacing with the FlightGear flight simulator.

* Download the complete package (simulator + controller design) at `http://www.ims-bordeaux.fr/images/IFAC_WC2020_HL20.zip` and read the file "ToDo.txt".

Keywords: H_∞-theory, MIMO control, aerospace applications.

NOTATIONS and NOMENCLATURE:
For a linear state space model (A, B, C, D), $P(s)$ (or simply P) is its associated Laplace transform. The notation $P(s) : \left[\begin{array}{c|c} A & B \\ \hline C & D \end{array}\right]$ is used in the paper. $P(s)$ is assumed to be in $\mathbb{R}H_\infty$, real rational function with $||P||_\infty = \sup_\omega \overline{\sigma}(P(j\omega)) < \infty$, where $\overline{\sigma}(M)$ denotes the maximum singular value of the matrix $M \in \mathbb{C}^{n\times m}$. $||P||_\infty$ is also called the H_∞-norm (or maximum gain) of P.

The following nomenclature is used:

α, β	= angle-of-attack and sideslip
ϕ, θ, ψ	= roll, pitch and yaw angles
p, q, r	= roll, pitch and yaw rates
x, y, h	= ground position of the vehicle
u_b, v_b, w_b	= 3-axis velocity components
V_{TAS}, $\overline{q}$	= true air speed, dynamic pressure
X_{cg}	= center of gravity coordinate
Ixx, Iyy, Izz	= moments of inertia about x,y,z-axis
$Cx_0(\alpha, \beta)$	= axial force coefficient
$Cy_0(\beta)$	= side force coefficient
$Cz_0(\alpha, \beta)$	= normal force coefficient
$Cl_0(\beta)$	= rolling moment coefficient
$Cm_0(\alpha, \beta)$	= pitching moment coefficient
$Cn_0(\alpha, \beta)$	= yawing moment coefficient
$\delta_{bfll}, \delta_{bflr}$	= lower left and right body-flap deflection
$\delta_{bful}, \delta_{bfur}$	= upper left and right body-flap deflection
$\delta_{wfl}, \delta_{wfr}$	= left and right winged-flap deflection
δ_r	= rudder deflection
m	= vehicle mass

1. THE H_∞ MIXED-SENSITIVITY APPROACH

The mixed sensitivity approach of the H_∞ problem consists in designing a controller to stabilize the closed loop system and achieve a good compromise between robustness and performances, considering constraints on the control signal (Zhou, Doyle, and Glover, 1996). This is ensured by a suitable choice of frequency weighting functions placed in specific locations on the control scheme.

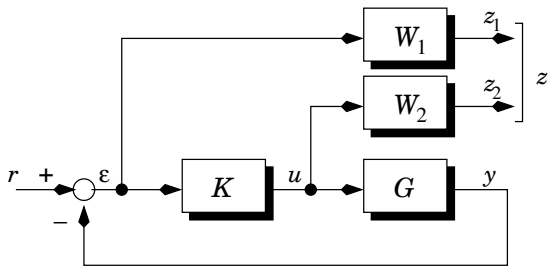

Fig. 1. Block diagram of the mixed sensitivity approach

To proceed, let us consider the multi-variable closed-loop system illustrated by the block diagram on Fig. 1 and let us denote (as classically) $S = (I + GK)^{-1}$ and $R = KS$ the so-called sensitivity function (representing the transfer from r to ε) and the command sensitivity function (representing the transfer from r to u). To take into account the closed loop performance objectives, the following constraint is imposed on S:

$$\overline{\sigma}\left(S(j\omega)\right) \leq |W_1^{-1}(j\omega)| \quad \forall\omega \tag{1}$$

W_1 (assumed to be invertible) is the desired constraint to be determined so that the controller K meets some *a priori* fixed performance in terms of e.g. time response, static error, module margin, robust stability.
To obtain a controller that satisfies such objectives without violating *a priori* known constraints on the control signal u, one requires that

$$\overline{\sigma}\left(R(j\omega)\right) \leq |W_2^{-1}(j\omega)| \quad \forall\omega \tag{2}$$

where W_2 (assumed to be invertible) is the desired constraint to be determined in accordance with the specification on $u(t)$. Typical constraints are minimising the energy

Copyright lies with the authors

$||u||_2$, preserving measurement noise amplification on the control signal $u(t)$ or control saturation.
Due to the property of the maximum singular values that states for two matrices $M_i \in \mathbb{C}, i = 1, 2$

$$\overline{\sigma}\left(\begin{bmatrix} M_1 \\ M_2 \end{bmatrix}\right) \leq \sqrt{2}\max\{\overline{\sigma}(M_1), \overline{\sigma}(M_2)\} \tag{3}$$

it is immediate to see that a sufficient condition for (1) and (2) to hold is

$$\|T_{zr}\|_\infty \leq 1 \quad T_{zr} = \begin{bmatrix} W_1 S \\ W_2 R \end{bmatrix} \tag{4}$$

This H_∞ problem, called the mixed sensitivity problem (Kwakernaak, 1993), is a sub-optimal problem as opposed to the joint objectives (1) and (2), but due to (3), the sub-optimal solution is close to $\sqrt{2}$ to the optimal solution.

Equation (4) demonstrates that the initial block diagram of Fig. 1 can be reformulated according to the diagram given in Fig. 2, which is referred as the H_∞ standard problem. On Fig. 2, P is the augmented system that contains G and the weights $W_i, i = 1, 2$.

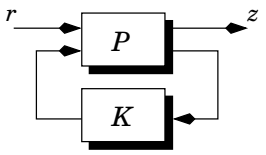

Fig. 2. The H_∞ standard problem

The H_∞ control problem can then be stated as follows. Given a real rational transfer matrix $P(s)$, and a space $\mathcal{K}$ of real rational transfer matrices $K(s)$, called the controller space, characterize and compute an optimal solution $K^* \in \mathcal{K}$ to the following optimization problem

$$\begin{aligned} &\text{minimize } \gamma \\ &\text{subject to } \; K \text{ stabilizes } P \text{ internally} \\ &\qquad\qquad K \in \mathcal{K}, \|T_{zr}\|_\infty \leq \gamma \end{aligned} \tag{5}$$

Then it is obvious to see that, if the optimal value γ^* is strictly less than 1, then we have found a controller K that fulfils (1) and (2). However, due to (3), a value of $\gamma^* : \gamma^* \leq \sqrt{2}$ does not necessarily lead to a non viable controller K, since (1) and (2) can be satisfied. That is why, practically, if $1 \leq \gamma^* \leq \sqrt{2}$, constraints (1) and (2) are *a posteriori* checked.

As we shall see from (5), the choice of the controller space $\mathcal{K}$ in (5) is the key for a proper understanding of the problem. Let us define the following notations

$$P(s) : \left[\begin{array}{c|cc} A & B_1 & B_2 \\ \hline C_1 & D_{11} & D_{12} \\ C_2 & D_{21} & D_{22} \end{array}\right] \quad K(s) : \left[\begin{array}{c|c} A_K & B_K \\ \hline C_K & D_K \end{array}\right] \tag{6}$$

with $A \in \mathbb{R}^{n\times n}, B_2 \in \mathbb{R}^{n\times n_u}, C_2 \in \mathbb{R}^{n_y\times n}$ and $A_k \in \mathbb{R}^{k\times k}$. The so-called "full-order controller" solution behaves to the solutions within of the space $\overline{\mathcal{K}}$ defined by

$$\overline{\mathcal{K}} = \{K : K \text{ has the form (6) with } k = n\} \tag{7}$$

Note that in $\overline{\mathcal{K}}$, all entries in A_K, B_K, C_K, D_K are free variables and thus we have $N = n^2 + n(n_y + n_u) + n_y n_u$ degrees of freedom. In particular, $\overline{\mathcal{K}}$ is the largest controller space which is convex. Finding a solution within $\overline{\mathcal{K}}$ can then be done by using an optimisation algorithm.

In (Glover and Doyle, 1988), it is shown that solving this optimisation problem requires the solution of two algebraic Riccati equations (AREs). This solution has been implemented in a matlab function called "*hinfsyn*". In (Gahinet and Apkarian, 1994), the authors establish a solution by reducing (5) to a semi definite programming problem, i.e. an optimization problem under linear matrix inequality (LMI) constraint. This solution has been implemented in a matlab function called "*hinflmi*". In this training paper, we use the LMI-based solution and we invite the interested reader to refer to (Gahinet and Apkarian, 1994).

Remark 1. The general formulation of the H_∞ mixed-sensitivity approach considers a constraint on the complementary function $T = \mathbb{I} - S$ (representing the transfer from r to y) such that $\overline{\sigma}(T(j\omega)) \leq |W_3^{-1}(j\omega)| \, \forall\omega$. We argue in this training paper that if S and R are correctly constrained, then considering W_3 is useless, simply because $S + T = \mathbb{I}$ implies $|W_1^{-1}(j\omega)| + |W_3^{-1}(j\omega)| > 1 \, \forall\omega$, which highlights that W_1 and W_3 are coupled.

2. APPLICATION TO THE HL-20 VEHICLE

2.1 Problem statement

The required software package, is the software Matlab/Simulink with the AEROSPACE's toolbox. Once Matlab is launched, the HL-20 simulator is accessible by typing `"aeroblk_HL20"`, see Fig. 3.a. To prepare the implementation of the H_∞-controller, it is required to change the inner loop on the angular rates of the called *"classical controller"*, by a MIMO controller as depicted in Fig. 3.b. For easy implementation, a "`LTI System`" object can be used, with the variable "K", that will be defined through the Matlab instruction (we use the same notations than those of section 1 for easy reference):

$$K = \texttt{ss(AK,BK,CK,DK)}$$

The resulting control law is then a standard guidance, navigation and control (GNC) system, dedicated to the auto-landing phase, whose angular rates will be controlled by the H_∞ controller K. The guidance algorithm ensures the tracking of the auto-landing reference trajectory which is computed by the path planner. The guidance commands $\phi_{ref}, \alpha_{ref}, \beta_{ref}$ (referred as "`Demands`" on Fig. 3.b) are the inputs to the attitude control loop which computes the control torques providing conventional rudder (d_r), aileron (d_a) and elevator (d_e) authorities. These signals are next converted into the actuator control input vector $\delta = [\delta_{wfl}, \delta_{wfr}, \delta_{ulbf}, \delta_{urbf}, \delta_{llbf}, \delta_{lrbf}, \delta_r]^T$ by means of a dedicated pressure-dependant allocation control algorithm, i.e. $\delta = M(\overline{q}_m)u$. The index "$m$" is used to outline that we speak about a measured signal, as opposed to its associated state where "m" is not used. δ is then applied to the actuators which are modelled as 2nd order transfer functions, with magnitude and slope saturations.

Information on body angular rates are supplied by an IMU and a Airdata system provides information on the angle-of-attack (AoA), angle-of-sideslip (AoS), True Air Speed velocity and $\overline{q}$. The ground position of the vehicle is given by a GPS and a Radar Altimeter system, see Fig. 3.a

Following 3.b, the control vector $u = (d_a \, d_e \, d_r)^T$ is given, in the Laplace domain, by:

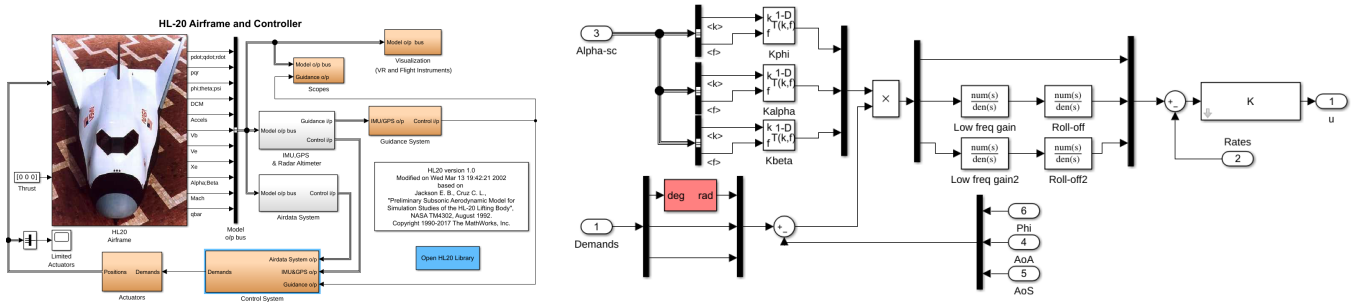

Fig. 3. (a). The HL-20 simulator (left) - (b). The inner loop on the angular rates of the classical controller (right)

$$u = K\left(K'k(\alpha_m)\begin{pmatrix}\phi_{ref}-\phi_m\\ \alpha_{ref}-\alpha_m\\ \beta_{ref}-\beta_m\end{pmatrix}-\begin{pmatrix}p_m\\ q_m\\ r_m\end{pmatrix}\right) \tag{8}$$

On Fig. 3.b, α_m is referred as "`Alpha-sc`", p_m, q_m, r_m are the vector denoted "`Rates`" and $K'(s)$ consists of the MIMO filter composed by the low frequency and roll-off transfers.

Following the method explained in section 1, the design of the H_∞ controller K is based on the following steps:

1) Establish the model G seen by K. In our case, we look for the model that links the control signals d_a, d_e, d_r to the angular rates p, q, r.
2) Determine the objective functions W_1 and W_2 based on some *a priori* fixed control performance.
3) Synthesise the controller K.

2.2 Step 1: towards the model G

Modelling the HL-20: The flight dynamics of the HL-20 winged body vehicle is derived from the classical 6 degree-of-freedom equations of motions of a symmetrical rigid aircraft. Under the assumptions of a flat and non rotating earth, which is implicit for the auto-landing trajectory duration, the rotational dynamics of the HL20 can be derived from the Euler's laws for symmetrical aircraft that is:

$$\begin{bmatrix}\dot p\\ \dot q\\ \dot r\end{bmatrix} = I^{-1}\left(M^{(b)}_{aero}-\begin{bmatrix}p\\ q\\ r\end{bmatrix}\wedge\left(I.\begin{bmatrix}p\\ q\\ r\end{bmatrix}\right)\right) \tag{9}$$

where the notation $\bullet^{(b)}$ is used to refer to the so-called "*body frame*". I is the inertia matrix, which is diagonal in our case, i.e. $I = diag(I_{xx}, I_{yy}, I_{zz})$. $\overrightarrow{M}^{(b)}_{aero} = L\overrightarrow{x}_b + M\overrightarrow{y}_b + N\overrightarrow{z}_b$ refers to the external torques vector acting on the vehicle. It consists of the aerodynamic torques due to the aero-surfaces deflections and to the aerodynamic induced torques.

The vehicle translational motion in the body coordinate frame can be written according to

$$\begin{bmatrix}\dot u\\ \dot v\\ \dot w\end{bmatrix} = \frac{1}{m}\left(F^{(b)}_{aero}+F^{(b)}_{g}\right)-\begin{bmatrix}p\\ q\\ r\end{bmatrix}\wedge\begin{bmatrix}u\\ v\\ w\end{bmatrix} \tag{10}$$

m is the total mass of the vehicle, $\overrightarrow{F}^{(b)}_{aero} = X_{aero}\overrightarrow{x}_b + Y_{aero}\overrightarrow{y}_b + Z_{aero}\overrightarrow{z}_b$ refers to the aerodynamic forces acting on the vehicle and $\overrightarrow{F}^{(b)}_{g} = F_{xg}\overrightarrow{x}_b + F_{yg}\overrightarrow{y}_b + F_{zg}\overrightarrow{z}_b$ refers to the gravity vector, all given in the body frame.

The kinematic equations that link the so-called Euler angles ϕ, θ, ψ to angular velocities p, q, r are given by

$$\begin{bmatrix}\dot\phi\\ \dot\theta\\ \dot\psi\end{bmatrix} = \begin{pmatrix}1 & s_\phi t_\theta & c_\phi t_\theta\\ 0 & c_\phi & -s_\phi\\ 0 & -s_\phi/c_\theta & -c_\phi/c_\theta\end{pmatrix}\begin{bmatrix}p\\ q\\ r\end{bmatrix} \tag{11}$$

where $c_\bullet, s_\bullet, t_\bullet$ refer to the functions $cos(\bullet), sin(\bullet), tan(\bullet)$ respectively. The positions of the vehicle x, y, z (with $h = -z$) in the Earth centred frame are given by

$$\begin{bmatrix}\dot x\\ \dot y\\ \dot z\end{bmatrix} = R^e_b\begin{bmatrix}u\\ v\\ w\end{bmatrix} \tag{12}$$

where R^e_b denotes the coordinate change matrix between body frame and the Earth centred frame, i.e.

$$R^e_b = \begin{pmatrix}c_\theta c_\psi & s_\phi c_\theta c_\psi - c_\phi s_\psi & c_\phi s_\theta c_\psi + s_\phi s_\psi\\ c_\theta s_\psi & s_\phi s_\theta s_\psi + c_\phi c_\psi & c_\phi s_\theta s_\psi - s_\theta c_\psi\\ -s_\theta & s_\phi c_\theta & c_\phi c_\theta\end{pmatrix} \tag{13}$$

Using the Bernoulli principle, the above introduced torques and forces are given by (in the body frame)

$$\begin{aligned}
&L = \overline{q}SbC_l(\alpha,\beta,V,r,p,\delta^*)\\
&M = \overline{q}S\overline{c}C_m(\alpha,\beta,q,V,\delta^*) + C_z(\alpha,\beta,\delta^*)(X_{cp}-X_{cg})\\
&N = \overline{q}SbC_n(\alpha,\beta,p,q,V,\delta^*) - C_y(\alpha,\beta,\delta^*)(X_{cp}-X_{cg})\\
&F_x = X_{aero}+F_{gx} = \overline{q}SC_x(\alpha,\beta,\delta^*) - mgs_\theta\\
&F_y = Y_{aero}+F_{gy} = \overline{q}SC_y(\alpha,\beta,\delta^*) + mgs_\theta c_\theta\\
&F_z = Z_{aero}+F_{gz} = \overline{q}SC_z(\alpha,\beta,\delta^*) + mgc_\theta c_\phi
\end{aligned} \tag{14}$$

C_l, C_m, C_n, C_x, C_y and C_z correspond to the dimensionless aerodynamic coefficients, that are also stored through look-up tables. $\delta^* = [\delta_a, \delta_e, \delta_r, \delta_{f^+}, \delta_{f^-}, \delta_{\Delta_f}]^T$ is the aerodynamic command vector that is deduced from the control surfaces command vector δ so that:

$$\delta^* = \begin{bmatrix}0.5 & -0.5 & 0 & 0 & 0 & 0 & 0\\ 0.5 & 0.5 & 0 & 0 & 0 & 0 & 0\\ 0 & 0 & 0 & 0 & 0 & 0 & 1\\ 0 & 0 & 0 & 0 & 0.5 & 0.5 & 0\\ 0 & 0 & 0.5 & 0.5 & 0 & 0 & 0\\ 0 & 0 & 0.5 & -0.5 & 0.5 & -0.5 & 0\end{bmatrix}\delta \tag{15}$$

Numerical values of S, $\bar c$, b, X_{cp} X_{cg}, m are in the HL-20 simulator. $\overline{q} = \frac{1}{2}\rho SV^2$ where $\rho = \rho_0 \exp^{-z/H}$ with $H = 7100m$ is the air density. $\rho_0 = 1,293Kg/m^3$ is the sea level standard air density. g denotes the gravity constant.

Let us denote u_w, v_w, w_w the component of the wind and atmospheric turbulences along the three axes $\overrightarrow{x}_b$, $\overrightarrow{y}_b$, $\overrightarrow{z}_b$, it follows that

$$V = \sqrt{(u-u_w)^2 + (v-v_w)^2 + (w-w_w)^2} \quad (16)$$

$$\alpha = \arctan\left(\frac{w-w_w}{u-u_w}\right) \quad \beta = \arcsin\left(\frac{v-v_w}{V}\right) \quad (17)$$

As classically done in the aerospace community, $u_w(t)$, $v_w(t)$, $w_w(t)$ are modelled by means of Dryden filters.

Mathematical expression of the aerodynamic coefficients: A key feature consists now, in obtaining a mathematical description of the aerodynamic coefficients C_l, C_m, C_n, C_x, C_y and C_z. To proceed, let us first remark that $C_{aero} = [C_x, C_y, C_z, C_l, C_m, C_n]^T = \sum_{i=0}^{7} C_i$ where the terms $C_i, i = \overline{1,7}$ are given by (18).

As it can be seen, the components of C_{aero} mainly consist of two kinds of terms: i) the aerodynamic components depending uniquely on the angle-of-attack α, say the 1-dimensional coefficients and ii) the aerodynamic terms having a dependency with angle-of-attack α and the angle-of-sideslip β . These latter coefficients are thus 2-dimensional coefficients. Towards this end, the following modelling approach are used:
i) For the 1-dimensional coefficients, a least-square polynomial interpolation technique allows to derive analytical expressions such that:

$$\hat{C}_j = \sum_{k=0}^{n} a_{jk}\rho^k, \quad \rho = \{\alpha, \beta\}, \quad \max(n) = 6$$
$$j = \left\{ \begin{array}{l} y_0, l_\beta, x_{\delta_e}, z_{\delta_e}, m_{\delta_e}, x_{\Delta f}, y_{\Delta f}, l_{\Delta f}, n_{\Delta f} \\ x_{f+}, z_{f+}, m_{f+}, x_{f-}, z_{f-}, m_{f-}, x_{\delta_r}, y_{\delta_r} \\ z_{\delta_r}, l_{\delta_r}, m_{\delta_r}, n_{\delta_r}, x_{\delta_a}, y_{\delta_a}, z_{\delta_a}, l_{\delta_a} \\ m_{\delta_a}, n_{\delta_a}, l_p, n_p, m_q, l_r, n_r \end{array} \right\} \quad (19)$$

ii) Referring to the 2-dimensional coefficients in clean configuration, a principal component analysis method is used, that is

$$\left\{ \begin{array}{l} \hat{C}_{j0}(\alpha,\beta) = \overline{\sigma}(C_{j0}(\alpha,\beta))\hat{u}_{(:,1),j}(\alpha)\hat{v}_{(:,1),j}(\beta) \\ j = \{x, z, m, n\} \end{array} \right. \quad (20)$$

where $\hat{u}_{(:,1),j} = \sum_{l=0}^{6} a_{jl}\alpha^l$ and $\hat{v}_{(:,1),j} = \sum_{v=0}^{6} b_{jv}\beta^v$ correspond to polynomial approximations (in the least square sense) of the left and right singular vectors associated to $\overline{\sigma}(C_{j0}(\alpha,\beta))$, the maximum singular value of $C_{j0}(\alpha,\beta)$.

To validate these models, the aerodynamic coefficients provided by the look-up tables are superimposed with those computed by equations (19) and (20), see Fig. 4 where the example for C_{x0} is provided. As it can be seen, an approximation error remains. However, we argue that this error can be adequately covered by imposing sufficient performance and stability margins to K.

Determination of G: Using the above derived models of the aerodynamic coefficients and joining equations (9)-(20) together, one can derive the following nonlinear state space model (the measurement noise, the wind and turbulence models are ignored from now on since they are not required to derive G):

$$\begin{array}{l} \dot{x_b} = f(x_b, u, \overline{q}) \\ y = Cx_b \end{array} \quad (21)$$

Then, by performing a linear approximation of (21) around the flight trajectory described by $(x_{b_{ref}}(t), u_{ref}(t))$, one can derive the following (approximated) linear parameter varying state space model

$$\begin{array}{l} \dot{x_b} = A(x_{b_{ref}}, u_{ref}, \overline{q})x_b + B(x_{b_{ref}}, u_{ref}, \overline{q})u \\ y = Cx_b \end{array} \quad (22)$$

$A(x_{b_{ref}}, u_{ref}, \overline{q})$ and $B(x_{b_{ref}}, u_{ref}, \overline{q})$ are matrices of appropriate dimensions. Expressing $x_{b_{ref}}, u_{ref}$ and $\overline{q}$ as functions of the reference flight velocity V_{ref} and selecting the adequate measurements (i.e. p, q, r), it follows that the model we are looking for is given by

$$G(V_{ref}) : \left\{ \begin{array}{l} \dot{x_b} = A(V_{ref})x_b + B(V_{ref})u \\ [p \ q \ r]^T = NCx_b \end{array} \right. \quad (23)$$

where N is a matrix that selects p, q, r. Considering the slow variation of V_{ref} during the auto-landing phase (no abrupt acceleration or deceleration), $G(V_{ref}) = G$ remains a family of LTI models, each model of this family corresponding to a fixed V_{ref}. Fig. 5 illustrates the principals gain ("singular value plot") for a sufficient dense gridding of V_{ref} over the overall landing trajectory. From these figures, it can be seen that K must be designed to be robust to the variations of G induced by V_{ref}.

For that purpose, the following strategy is used:
i) first, K is designed based on a unique model computed at a judiciously chosen speed V_{ref}, i.e. $V_{ref} = 135m/s$;
i) second, the ability of K to satisfy the required control performance $\forall V_{ref}$, is checked using (23).

2.3 Step 2: Determination of W_1 and W_2

With regards to W_1, since there does not exist *a priori* justifications to control the vehicle along its 3 axis with different performance, it is chosen as:

$$W_1^{-1}(s) = C_1 \frac{s+\omega_l}{s+\omega_u}\mathbb{I}_3 \quad \omega_l \ll \omega_u \quad (24)$$

ω_u refers to the bandwidth of the closed loop and ω_l is a frequency introduced to make W_1 invertible that can be chosen arbitrarily. Since $\lim_{\omega\to 0} |W_1^{-1}(j\omega)| = C_1\frac{\omega_l}{\omega_u}$, the smallest ω_l is, the smallest will be the static error since W_1^{-1} (and thus S) will have small gain. With regards to C_1, since it is nothing else than the high frequency gain of W_1^{-1}, it represents the constraint on the module margin. It is then chosen to $C_1 = 2$ ($\approx 6dB$). The remaining problem is then the determination of ω_u. A fundamental issue in designing a controller is to manage adequately the effect of the measurement noise $n(t)$ on the control signal $u(t)$. Especially, a high value of ω_u implies a high amplification of $n(t)$ on $u(t)$. Thus, determining ω_u is strictly equivalent to determining the maximum amplification of $n(t)$ that is tolerated on $u(t)$.

To solve this problem, let us first come back to the theory of SISO control. With the same notations than used previously, the transfer between the measurement noise n and the control signal is given by $\frac{u}{n} = \frac{-K}{1+GK}$. Assuming that K is a correctly designed controller, K has high gain in low frequencies (thanks for instance to its integral component). Generally, G has no gain in high frequencies (this is the case there, see Fig. 4.b). Furthermore, K has constant or no gain in high frequencies. It follows that

$$C_0 = \begin{bmatrix} C_{x0}(\alpha,\beta) \\ C_{y0}(\beta) \\ C_{z0}(\alpha,\beta) \\ C_{l\beta}(\beta) \\ C_{m0}(\alpha,\beta) \\ C_{n0}(\alpha,\beta) \end{bmatrix}, C_1 = \begin{bmatrix} C_{x_{\delta_a}}(\alpha).|\delta_a| \\ C_{y_{\delta_a}}(\alpha).\delta_a \\ C_{z_{\delta_a}}(\alpha).|\delta_a| \\ C_{l_{\delta_a}}(\alpha).\delta_a \\ C_{m_{\delta_a}}(\alpha).|\delta_a| \\ C_{n_{\delta_a}}(\alpha).\delta_a \end{bmatrix}, C_2 = \begin{bmatrix} C_{x_{\delta_e}}(\alpha).\delta_e \\ 0 \\ C_{z_{\delta_e}}(\alpha).\delta_e \\ 0 \\ C_{m_{\delta_e}}(\alpha).|\delta_e| \\ 0 \end{bmatrix}, C_3 = \begin{bmatrix} C_{x_{\delta_r}}(\alpha).|\delta_r| \\ C_{y_{\delta_r}}(\alpha).\delta_r \\ C_{z_{\delta_r}}(\alpha).|\delta_r| \\ C_{l_{\delta_r}}(\alpha).\delta_r \\ C_{m_{\delta_r}}(\alpha).|\delta_r| \\ C_{n_{\delta_r}}(\alpha)\delta_r \end{bmatrix} \forall\alpha \geq 0,\ C_4 = \begin{bmatrix} C_{x_{\delta_{f+}}}(\alpha).\delta_{f+} \\ 0 \\ C_{z_{\delta_{f+}}}(\alpha).\delta_{f+} \\ 0 \\ C_{m_{\delta_{f+}}}(\alpha).|\delta_{f+}| \\ 0 \end{bmatrix}$$

$$C_5 = \begin{bmatrix} C_{x_{\delta_{f-}}}(\alpha).\delta_{f-} \\ 0 \\ C_{z_{\delta_{f-}}}(\alpha).\delta_{f-} \\ 0 \\ C_{m_{\delta_{f-}}}(\alpha).|\delta_{f-}| \\ 0 \end{bmatrix}, C_6 = \begin{bmatrix} C_{xd\Delta f}(\alpha).|\delta_{\Delta f}| \\ C_{y_{\Delta f}}(\alpha).\delta_{\Delta f} \\ 0 \\ C_{l_{\Delta f}}(\alpha).\delta_{\Delta f} \\ 0 \\ C_{n\Delta f}(\alpha)\delta_{\Delta f} \end{bmatrix}, C_7 = \left(\frac{b.p}{2V} \begin{bmatrix} 0 \\ 0 \\ 0 \\ C_{lp}(\alpha) \\ 0 \\ -C_{np}(\alpha) \end{bmatrix} + \frac{\bar{c}.q}{2V} \begin{bmatrix} 0 \\ 0 \\ 0 \\ 0 \\ C_{mq}(\alpha) \\ 0 \end{bmatrix} + \frac{b.r}{2V} \begin{bmatrix} 0 \\ 0 \\ 0 \\ C_{lr}(\alpha) \\ 0 \\ C_{nr}(\alpha) \end{bmatrix} \right) \tag{18}$$

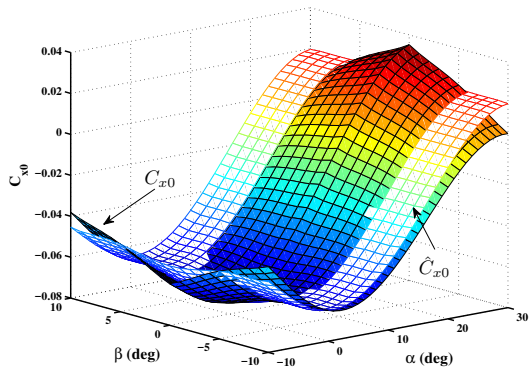

Fig. 4. C_{x0} an $\hat{C}_{x0}$

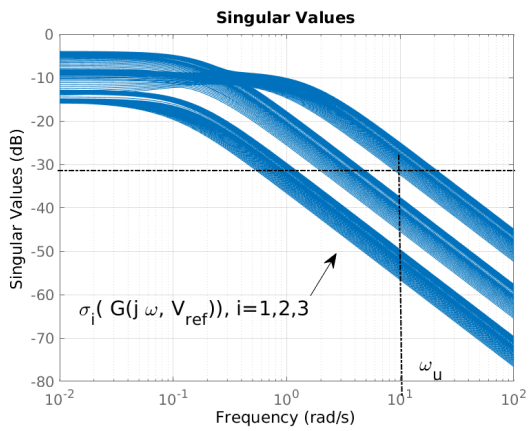

Fig. 5. $\sigma_i\left(G(j\omega, V_{ref})\right)$

(the sign is ignored since only the gain is interest for our reasoning):

$$\frac{u}{n} \approx \frac{1}{G}\ \forall\omega \ll \omega_u \text{ and } \frac{u}{n} \approx K\ \forall\omega \gg \omega_u \tag{25}$$

For a PID controller with $50^o - 60^o$ of phase margin, we know that between these two frequency ranges (i.e. those that conatin ω_u), the bode diagram of $\frac{K}{1+GK}$ does not "overshoot" $15dB$ from $\frac{1}{G}$. Thus, determining admissible values for ω_u can be derived knowing the maximum values n_{max} and u_{max} of n and u:

$$\omega_u = \omega : \left|\frac{1}{G(j\omega)}\right|_{dB} \lessapprox \left|\frac{u_{max}}{n_{max}}\right|_{dB} - 15dB \tag{26}$$

This reasoning can be extended to MIMO systems, replacing $|G(j\omega)|$ by $\overline{\sigma}(G(j\omega))$. Thus, for the case of the HL-20, since $i)$ the measurement noise on p, q, r provided by the IMU does not exceed $0.01^o/s$ and $ii)$ the amplification of this noise on $u = [d_a\ d_e\ d_r]^T$ is fixed to 2° max, $ii)$ G depends on V_{ref}, it follows with the help of the Fig. 5 that ω_u if fixed to $\omega_u = 10rd/s$.

With regards to W_2, it is chosen according to

$$W_2^{-1}(s) = C_2 \frac{1 + 1/\omega_h s}{1 + 1/\omega_c s} \mathbb{I}_3 \quad \omega_h \gg \omega_c \tag{27}$$

ω_h is a frequency introduced to make W_2 invertible and can be chosen arbitrarily. Noting that the term $\frac{C_2}{1+1/\omega_c s}$ describes a low pass-filter of static gain C_2 with cutting frequency ω_c, it follows that minimizing both C_2 and ω_c enables to minimize the energy of the control commands $||u||_2$ over the largest frequency range possible.

2.4 Step 3: Design of K

The controller K is next computed using the theory described in section 1. For that purpose,the block diagram illustrated on Fig. 1 is drawn using Simulink. The controller K is of course removed, since it is looked for. The model P is then derived using the "`linmod`" Matlab code. Next, the "`hinflmi`" function is used to compute K. This results in the following Matlab's sequence code:

```
[AP,BP,CP,DP]=linmod(file_name);
P=pck(AP,BP,CP,DP);
[gopt,K] = hinflmi(P,[3 3]);
[AK,BK,CK,DK]=unpck(K);
```

Then, the ability of the so computed K to satisfy the required control performance specified by W_1 and W_2 are checked for a dense gridding of V_{ref}. Fig. 6.a and 6.b illustrate the results. Clearly, it can be seen that the robust control requirements are satisfied since $\overline{\sigma}\left(S(j\omega, V_{ref})\right) \leq |W_1^{-1}(j\omega)|, \forall(\omega, V_{ref})$ and $\overline{\sigma}\left(R(j\omega, V_{ref})\right) \leq |W_2^{-1}(j\omega)|, \forall(\omega, V_{ref})$.

2.5 Nonlinear simulation results

The controller K is finally implemented in the HL-20 simulator as illustrated on Fig. 3.b. The simulator is next interfaced with FlightGear flight simulator [1] using

[1] www.flightgear.org

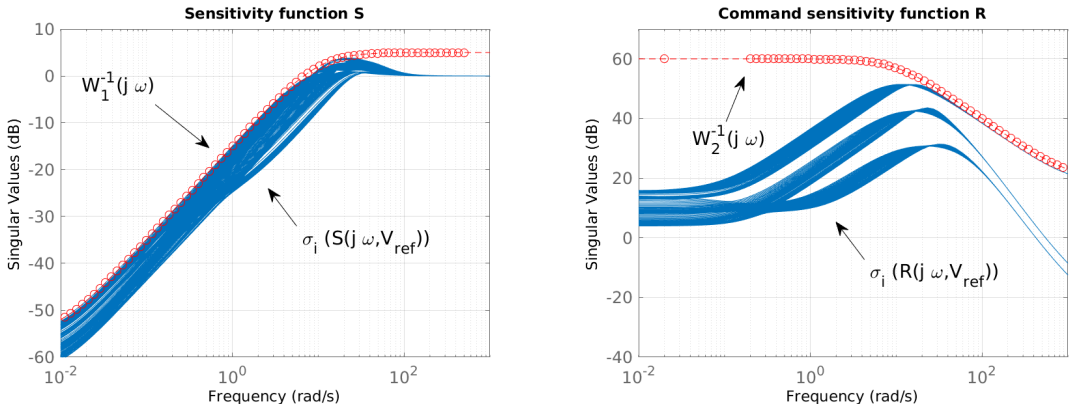

Fig. 6. (a): Sensitivity function $S(V_{ref})$ vs W_1^{-1} (left) - (b): Control sensitivity function $R(V_{ref})$ vs W_2^{-1} (right)

the Matlab AEROSPACE toolbox facilities. Fig. 7 illustrates the behaviour of the roll angle $\phi(t)$, angle-of-attack $\alpha(t)$, angle-of-sideslip $\beta(t)$ versus their references $\phi_{ref}(t), \alpha_{ref}(t), \beta_{ref}(t)$ provided by the guidance loop. Fig. 8 gives the behaviour of the control signal $u(t) = [d_a(t)\ d_e(t)\ d_r(t)]^T$. Finally Fig. 9 gives an illustration coming from FlightGear. As it can be seen, the controller K is able to control the HL-20 so that the vehicle can land autonomously.

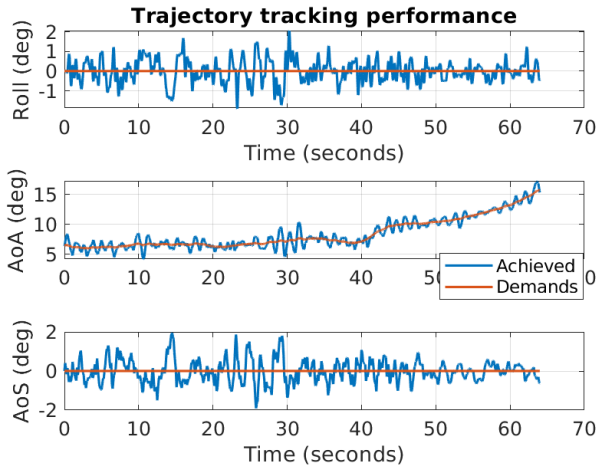

Fig. 7. $\phi(t)$, $\alpha(t)$ and $\beta(t)$

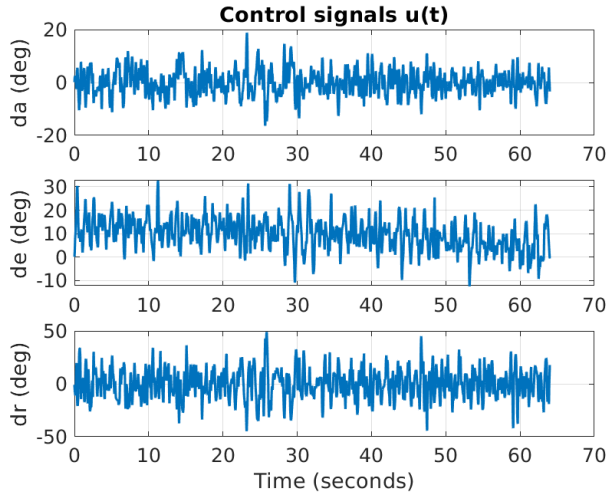

Fig. 8. control signal $u(t)$

Fig. 9. Flightgear illustration

3. CONCLUSION

This paper investigated the application of the mixed-sensitivity approach of the robust H_∞ control theory, to the auto-landing phase of a re-entry mission. The paper covers all the aspect of the engineer exercise, i.e. from establishing the non-linear model of the vehicle, considering especially the mathematical description of the non-linear aerodynamic coefficients, until the implementation of the robust H_∞ controller in a GNC architecture. A particular attention is paid on the design of the frequency weighting functions that enable to correctly constraint the design of the controller. Simulation of the complete auto-landing phase, interfaced with the FlightGear flight simulator, should convince that the mixed-sensitivity approach of the robust H_∞ control theory is now a viable theory to be used in aerospace industries.

REFERENCES

Gahinet, P. and Apkarian, P. (1994). A linear matrix inequality approach to H_∞ control. *Int. Journal Robust Nonlinear Control*, 4, 421–428.

Glover, K. and Doyle, J. (1988). State-space formulae for all stabilizing controllers that satisfy an H_∞-norm bound and relations to risk sensitivity. *System and control letters*, 11, 167 – 172.

Kwakernaak, H. (1993). Robust control and h-optimizationtutorial paper. *Automatica*, 29(2), 255 – 273. doi:https://doi.org/10.1016/0005-1098(93)90122-A. URL `http://www.sciencedirect.com/science/article/pii/000510989390122A`.

Zhou, K., Doyle, J., and Glover, K. (1996). *Robust and Optimal Control*. Prentice Hall.